

“Light-cone” dynamics after quantum quenches in spin chains

Lars Bonnes,^{1,*} Fabian H. L. Essler,² and Andreas M. Läuchli¹

¹*Institute for Theoretical Physics, University of Innsbruck, A-6020 Innsbruck, Austria.*

²*The Rudolf Peierls Centre for Theoretical Physics, Oxford University, Oxford OX1 3NP, UK*

(Dated: September 10, 2018)

Signal propagation in the non equilibrium evolution after quantum quenches has recently attracted much experimental and theoretical interest. A key question arising in this context is what principles, and which of the properties of the quench, determine the characteristic propagation velocity. Here we investigate such issues for a class of quench protocols in one of the central paradigms of interacting many-particle quantum systems, the spin-1/2 Heisenberg XXZ chain. We consider quenches from a variety of initial thermal density matrices to the same final Hamiltonian using matrix product state methods. The spreading velocities are observed to vary substantially with the initial density matrix. However, we achieve a striking data collapse when the spreading velocity is considered to be a function of the excess energy. Using the fact that the XXZ chain is integrable, we present an explanation of the observed velocities in terms of “excitations” in an appropriately defined generalized Gibbs ensemble.

The last few years have witnessed a number of significant advances in understanding the nonequilibrium dynamics in isolated quantum systems. Much of this activity has focussed on fundamental concepts such as thermalization [1–5] or the roles played by dimensionality and conservation laws [6–16].

Another key issue concerns the spreading of correlations out of equilibrium, and in particular the “light-cone” effect after global quantum quenches. The most commonly studied protocol in this context is to prepare the system in the ground state of a given Hamiltonian, and to then suddenly change a system parameter such as a magnetic field or interaction strength. At subsequent times the spreading of correlations can then be analyzed by considering the time-dependence of two-point functions of local operators separated by a fixed distance. As shown by Lieb and Robinson [17, 18], the velocity of information transfer in quantum systems is bounded. This gives rise to a causal structure in commutators of local operators at different times, although Schrödinger’s equation, unlike relativistic theories, has no built-in speed limit. Recently, the Lieb-Robinson bounds have been refined [19–21] and extended to mixed state dynamics in open quantum systems [21, 22] as well as creation of topological quantum order [23].

A striking consequence of the Lieb-Robinson bound is that the equal-time correlators after a quantum quench feature a “light-cone” effect [23], which is most pronounced for quenches to conformal field theories from initial density matrices with a finite correlation length [24]: connected correlations are initially absent, but exhibit a marked increase after a time $t_0 = x/2v$. This observation is explained by noting [25, 26] that entangled pairs of quasi-particles initially located half-way between the two points of measurement, propagate with the speed of light v and hence induce correlations after a time t_0 . These predictions have been verified numerically in several systems, see e.g. [27–32]. Very recently light-cone effects after quantum quenches have been observed in systems of ultra-cold atomic gases [33, 34] and trapped ions [35, 36]. The experimental work raises the poignant theoretical issue of which velocity underlies the observed light-

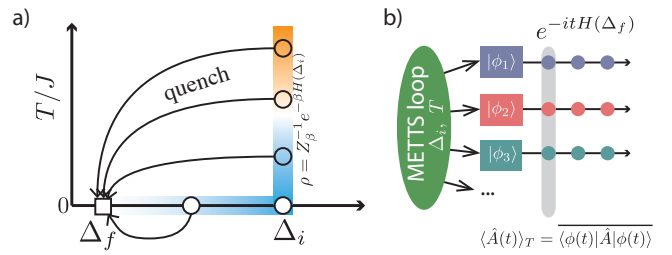


FIG. 1. (Color online) a) Quench protocol: The system is initially prepared in either the ground state of some Hamiltonian $H(\Delta_i)$ or in a thermal state $\rho = Z_\beta^{-1} \exp[-\beta H(\Delta_i)]$ with temperature $T = 1/(k_B \beta)$. At time 0, the anisotropy is quenched to Δ_f and we let the system evolve in time for various initial values of Δ_i and T . b) Outline of the numerical procedure: The METTS projection loop generates an ensemble of wave function for some initial Δ_i and temperature T . Each realization is evolved in time and expectation values are obtained by averaging over the ensemble.

cone effect in non-relativistic systems at finite energy densities. Here there is no unique velocity of light, and quasi-particles in interacting systems will generally have finite life times depending on the details of the initial density matrix.

In order to shed some light on this issue, we have carried out a systematic study of the spreading of correlations in the spin-1/2 Heisenberg XXZ chain, a key paradigm among interacting many body quantum systems in one spatial dimension. We fix the final (quenched) Hamiltonian and vary the initial conditions over a large range of parameters. Moreover, we do not only consider initial pure states [29] but also prepare the system in thermal initial states as illustrated in Fig. 1(a). The latter is of significant interest in view of experimental realizations. Apart from a recent numerical study for local quenches [37], the spreading of signals in quenches from thermal states is basically unexplored.

Our numerical simulations are based on a quench extension of a recently proposed algorithm utilizing an optimized wave function ensemble called Minimally Entangled Typical Thermal States (METTS) [38, 39] implemented within the matrix

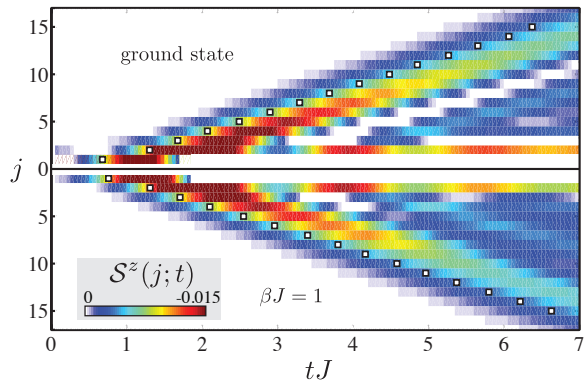


FIG. 2. Space-time plot of the \mathcal{S}^z correlation functions (3) for the quench from $\Delta_i = 4$ to $\Delta_f = \cos(\pi/4)$. This particular value of the final interaction is chosen due to technical reason in the Bethe ansatz calculations. The upper panel shows ground state data whereas the lower panel shows data from a thermal density matrix at $T/J = 1$. This illustrates that the light-cone effect in this observable persists also at finite temperatures.

product state (MPS) framework. We come back to the description of the algorithm and a discussion of its performance towards the end of this paper.

Results.— In the following we consider quenches to the spin-1/2 Heisenberg XXZ chain with anisotropy Δ

$$H(\Delta) = J \sum_{i=1}^{L-1} (S_i^x S_{i+1}^x + S_i^y S_{i+1}^y + \Delta S_i^z S_{i+1}^z). \quad (1)$$

Initially, the system is prepared in a Gibbs state corresponding to an XXZ Hamiltonian with anisotropy Δ_i at a temperature T , i.e.

$$\rho(t=0) = Z_\beta^{-1} \exp[-\beta H(\Delta_i)], \quad \beta = \frac{1}{k_B T}, \quad (2)$$

where $Z_\beta = \text{Tr} \exp[-\beta H(\Delta_i)]$ (we set $k_B = 1$). The anisotropy is then quenched at time $t = 0^+$ from Δ_i to $0 \leq \Delta_f \leq 1$, as depicted in Fig. 1(a), and the system subsequently evolves unitarily with Hamiltonian $H(\Delta_f)$ [40]. In order to probe the spreading of correlations we consider the longitudinal spin correlation functions

$$\mathcal{S}^z(j; t) = \langle S_{L/2}^z(t) S_j^z(t) \rangle - \langle S_{L/2}^z(t) \rangle \langle S_j^z(t) \rangle \quad (3)$$

centered around the middle of the chain. Results for $\mathcal{S}^z(j; t)$ are most easily visualized in space-time plots, and typical results are shown in Fig. 2. The most striking feature observed in these plots is the light-cone effect: at a given separation j connected correlations $\mathcal{S}^z(j; t)$ arise fairly suddenly at a time that scales linearly with j .

These results demonstrate that the light-cone effect persists for mixed initial states, although the visibility of the signal is diminished with increasing temperature (until it vanished completely at $\beta = 0$ since the initial density matrix is trivial

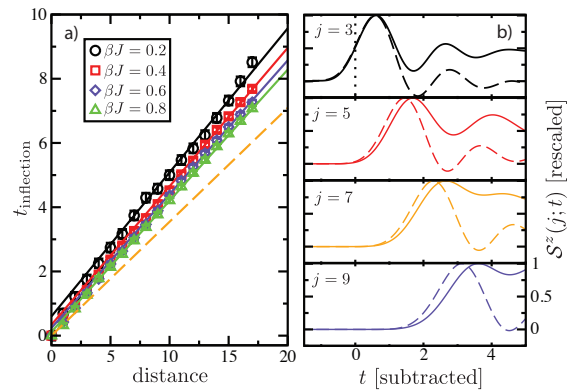


FIG. 3. *a)* Extracted inflection points versus distance for different initial temperatures for the quench from $\Delta = 4$ to $\cos(\pi/4)$. The straight lines correspond to the velocities extracted from the GGE where only the offset of the time axis has been fitted. The orange dashed line denotes the ground state Bethe ansatz velocity at Δ_f . *b)* Rescaled averaged spin correlation functions for the quench from $\Delta = 4$ to $\cos(\pi/4)$ for $T/J = 1$ and the ground state (dashed line) and different distances $j = 3, 5, 7$ and 9 . We omit the error bars for clarity of the figure. The time axis is relative to the first inflection point of the correlation functions for $j = 3$. One can see that the signal is delayed as the initial temperature is increased.

and stationary). Comparing the time evolution of the correlation functions for different initial temperatures, we see (cf Fig. 2 and Fig. 3) that the signal front is delayed when the temperature of the initial state is increased, signalling that the spreading slows down. We further observe that the spreading velocity is sensitive to the strength of the quench, i.e. the value of the initial interaction. At this point we should note that this finding is unexpected. Based on our current understanding of quenches to CFTs or of Lieb-Robinson bounds, there are no predictions available which support spreading velocities depending on the initial state.

Having established the result that the spreading velocity depends both on the initial density matrices and the final Hamiltonian, an obvious question is which properties of $\rho(t=0)$ are relevant in this context. In order to quantify this aspect we define the precise location of the light-cone as the first inflection point of the signal front observed in \mathcal{S}^z (alike Ref. 29). This allows us to extract a spreading velocity v_s by performing a linear fit to the largest accessible time, where expected finite-distance effects [41] are small.

Our main result, shown in Fig. 4, is that the spreading velocity is mainly determined by the *final energy density*

$$e_f = \frac{\text{Tr}[H(\Delta_f)\rho(t=0)]}{L}. \quad (4)$$

Plotting the measured velocities against e_f leads to a remarkable data collapse for a variety of quenches from thermal as well as pure initial states for various Δ_i . This holds in spite of the fact that the system is integrable and thus its dynamics is constrained by an infinite set of conserved quantities. As we will show in the following, the observed velocities can

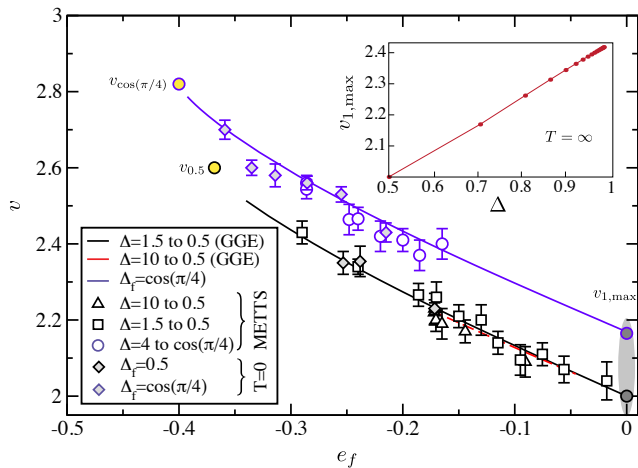


FIG. 4. (Color online) Spreading velocity v_s extracted from the spin correlation function \mathcal{S}^z as a function of the final energy e_f density for $\Delta_f = 1/2$ and $\cos \pi/4$. The symbols denote numerical results obtained from either thermal or pure initial states with different Δ_i . The blue and black solid lines denote the spreading velocities from TBA using only the energy density whereas the red line shows the results for the quench from $\Delta_i = 10$ to 0.5 using also the first conserved quantity. The corresponding velocities for the quench from $\Delta_i = 1.5$ lie on top of the black line, i.e. the GGE effects are smaller than the line width. The rightmost symbols denote v_{Δ_f} at the energy density of the ground state whereas the right most ones denote $v_{1,\max}$. The inset shows the velocity at $\beta = 0$, $v_{1,\max}$, extracted from the thermodynamic Bethe ansatz for $\Delta = \cos(\pi/n)$.

be explained quantitatively by considering “excitations” in an appropriately defined generalized Gibbs ensemble.

Focusing on the quenches to $\Delta_f = 1/2$ as well as $\cos(\pi/4) \approx 0.707$, we observe that the spreading velocity v_s decreases significantly as the final energy density is increased by increasing T or altering Δ_i . The numerical data suggests that v_s approaches a non-trivial velocity in the infinite-temperature limit that depends on Δ_f . In fact this velocity can be obtained from Bethe ansatz (see discussion below) and is shown for the series $\Delta_f = \cos(\pi/n)$ in the inset of Fig. 4. For very weak quenches, where only the low-energy (relative to the ground state of $H(\Delta_f)$) degrees of freedom become populated, one expects that the spreading velocity is given by the maximal mode velocity $v_\Delta = \pi[(1 - \Delta^2)/(2 \arccos \Delta)]^{-1/2}$. In fact, the spreading velocity extrapolates to v_{Δ_f} , when the final energy approaches the ground state energy of $H(\Delta_f)$. For the non-interacting case $\Delta_f = 0$ which reduces essentially to free fermions, we find that the spreading velocity for all initial conditions is compatible with the maximal mode velocity, $v_0 = 2$. This is consistent with results we obtained for quenches to the critical point of a one-dimensional Ising model in a transverse field, which is essentially also a free theory, where also no significant dependence of the spreading velocity on the initial conditions was observed.

We now provide a theoretical explanation of our striking numerical observations.

Excitations in a Generalized Gibbs Ensemble.— A recent work [42] proposed that correlation functions of local operators after a quench to an integrable model, prepared in a pure state $|\Psi\rangle$, are given by

$$\lim_{L \rightarrow \infty} \langle \mathcal{O}(t) \rangle = \lim_{L \rightarrow \infty} \left[\frac{\langle \Psi | \mathcal{O}(t) | \Phi_s \rangle}{2 \langle \Psi | \Phi_s \rangle} + \Phi_s \leftrightarrow \Psi \right]. \quad (5)$$

Here $|\Phi_s\rangle$ is a simultaneous eigenstate of the post-quench Hamiltonian and all local, higher conservation laws I_n , such that

$$i_n \equiv \lim_{L \rightarrow \infty} \frac{1}{L} \text{Tr}[\rho(t=0) I_n] = \lim_{L \rightarrow \infty} \frac{1}{L} \frac{\langle \Phi_s | I_n | \Phi_s \rangle}{\langle \Phi_s | \Phi_s \rangle}. \quad (6)$$

In the case of interest here we have $\mathcal{O}(t) = S_{L/2}^z(t) S_j^z(t)$. Importantly, the state $|\Phi_s\rangle$ can be constructed by means of a generalized Thermodynamic Bethe Ansatz (gTBA) [43, 44]. The stationary state itself is expected to be described by an appropriate GGE involving the known ultra-local [45] and quasi-local [46] conservation laws, and possibly others[47–51].

It was argued in Ref. 42 that states obtained by making microscopic changes to $|\Phi_s\rangle$ are most important to describe the dynamics at (sufficiently) late times. This is motivated by employing a Lehmann representation in terms of energy eigenstates $H(\Delta_f)|n\rangle = E_n|n\rangle$

$$\langle \Psi | \mathcal{O}(t) | \Phi_s \rangle = \sum_n \langle \Psi | n \rangle \langle n | \mathcal{O} | \Phi_s \rangle e^{-i(E_n - E_{\Phi_s})t}, \quad (7)$$

and noting that at sufficiently late times only states with $(E_n - E_{\Phi_s})/J = \mathcal{O}(1)$ are likely to contribute due to the otherwise rapidly oscillating phase. It is then tempting to conjecture that spreading of correlations occurs through these “excited states” (which by constructed can have either positive or negative energies relative to the representative state), and the light-cone effect propagates with the maximum group velocity that occurs amongst them. The method for calculating such excited state velocities is depicted schematically in Fig. 5, and details of the calculations are provided in the Supplementary Material. The basic idea is to use TBA methods to determine the macrostate minimizing the generalized Gibbs free energy. This is characterized by appropriate particle/hole distribution functions $\rho_j^{p,h}(x)$ for of elementary excitations labelled by the index j (x parametrizes the respective momenta). The corresponding “microcanonical” description [42, 52, 53] is based on the particular simultaneous eigenstate $|\Phi_s\rangle$ of the Hamiltonian and the higher conservation laws, characterized by the set $\{\rho_j^{p,h}(x)\}$ in the thermodynamic limit. One then considers small changes of this microstate, and determines the resulting $\mathcal{O}(1)$ (i.e. non-extensive) changes in energy and momentum. These can be described in terms of additive “elementary excitations” relative to $|\Phi_s\rangle$. Finally, one determines the dispersion relations and hence the group velocities of these excitations. The most significant qualitative features of the “GGE excitation spectrum” obtained in this way are as follows. (i) There are several types of infinitely long-lived elementary excitations. (ii) Their number depends only on the anisotropy

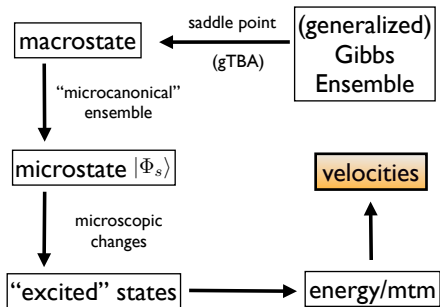


FIG. 5. Scheme for the extraction of the velocities from the GGE. See text for details.

Δ_f [54], but their dispersions are sensitive to the full set $\{i_n\}$ of (conserved) expectation values. (iii) In practice, we need to compute i_n numerically. Given that explicit expressions for I_n become rapidly extremely complicated [45], we retain only two conservation laws, namely energy and I_3 , which involves 4-spin interactions (I_2 is odd under time reversal and hence does not play a role for the quenches considered here). This can be justified by noting that the differences in the calculated maximal velocities between a Gibbs ensemble and a GGE with one added conservation law are small, and that the most local conservation laws are most important for accurately describing the properties of local operators [55]. (iv) In the cases we have considered, the maximal propagation velocity is found for the same type of excitation (“positive parity 1-strings”[54]). The results for the maximal velocities obtained from this gTBA analysis are compared to our numerical computations in the main panel of Fig. 4. The agreement is clearly very good. Also, the inset of Fig. 4 shows the velocities for infinite temperatures ($e_f = 0$) for $\Delta_f = \cos(\pi/n)$, where n is an integer, revealing a non-trivial Δ_f dependence even in this limiting case.

Numerical method.— After having provided the physical results we shortly review the numerical procedure employed to simulate the mixed state dynamics. MPS provide a powerful framework to study the real-time dynamics of one-dimensional quantum systems. Originally conceived for ground state calculations [56], extensions to finite temperatures include purification schemes [57–61], superoperators/matrix product operators (MPOs) [62–64] or transfer matrices [65–67]. Very recently Refs. [38, 39] introduced a stochastic method in which the expectation value of a thermal density matrix is replaced by an average over an ensemble of wave functions, $\{|\phi_i\rangle\}$, that *i*) can be efficiently sampled (importance sampling) using Markov chains and *ii*) only hosts the minimal (small) amount of entanglement required at that temperature, thus allowing for an efficient representation in terms of MPS. This ensemble was therefore called METTS (minimally entangled typical thermal states) [38, 39].

We show that the METTS method, thus far only applied to static equilibrium problems, can be easily extended to study

real time evolution by realizing that the expectation value of some real-time propagated operator $\hat{A}(t)$ can be written as

$$\langle \hat{A}(t) \rangle_T = \frac{1}{Z_\beta} \text{Tr} e^{-\beta H} \hat{A}(t) = \overline{\langle \phi_i(t) | \hat{A} | \phi_i(t) \rangle} \quad (8)$$

where the last term denotes an average over the time-evolved METTS ensemble [68]. We employ the numerical scheme illustrated in Fig. 1b) where we first generate an ensemble of wave functions following Ref. 39. In a second step each Φ_i is evolved in time using the TEBD algorithm [56] and Eq. (8) is evaluated. We average over a few hundred METTS instances and are limited due to runaway phenomena [69] to times of $tJ \sim 6 - 8$. Due to the reachable time scales we consider systems sizes of up to 50 sites here, but studying larger systems poses no particular problem by itself. A detailed description of the numerical method used here can be found in the Supplementary Material.

Compared to a complementary approach, where the von Neumann equation for the full system density matrix is integrated within an matrix product operator framework [62], we find that the METTS approach is able to reach significantly longer times, and we therefore believe that the METTS approach is quite promising to study global quenches at finite temperature. A full comparison of the different approaches, however, is beyond the scope of this paper and will be addressed in a forthcoming publication [70].

Conclusions.— We have analyzed the spreading of correlations after quantum quenches in the spin-1/2 Heisenberg XXZ chain. Our initial density matrix describing the system was taken to be a Gibbs distribution at a particular temperature and initial value of anisotropy Δ_i . We observed a pronounced light-cone effect in the connected longitudinal spin-spin correlation function. We found that the propagation velocity v of the light-cone depends not only on the final Hamiltonian, but also on the initial density matrix. For the quenches we considered the observed values of v are well-characterized by the expectation value of the final Hamiltonian in the initial state. These findings were found to be in accord with expectation based on properties of “excitations” in an appropriately defined generalized Gibbs ensemble. We also have shown that one can apply the METTS framework to study dynamical properties using MPS. Although the method also exhibits the typical runaway behavior, the lack of ancillary degrees of freedom or enlarged local Hilbert spaces reduces the complexity of the simulations and a direct comparison to other methods will be provided in a separate publication [70].

Our work raises a number of interesting issues. First, we expect that a full characterization of v will involve not only the final energy density, but the densities of all final higher conservation laws as well. In fact, we observe that the effects of higher conserved quantities are much more pronounced for negative Δ_f and this point is under investigation. Second, our work raises the question, whether horizon effects related to slower excitations can become visible for particular initial density matrices (in the case of local quenches this is indeed the case [71]). Finally, our work suggests that light-cone prop-

agation in generic non-integrable models ought to be rather non-trivial and warrants detailed investigation.

Acknowledgements.— We thank S. R. Manmana for discussions and acknowledge R. Bartenstein for collaboration at an early stage of the project. This work was supported by the Austrian Ministry of Science BMWF as part of the Uni-Infrastrukturprogramm of the Forschungsplattform Scientific Computing at LFU Innsbruck, by the FWF SFB FOQUS and by the EPSRC under grants EP/I032487/1 and EP/J014885/1.

* lars.bonnes@uibk.ac.at

- [1] M. Rigol, V. Dunjko, and M. Olshanii, *Nature* **452**, 854 (2008).
- [2] J. M. Deutsch, *Phys. Rev. A* **43**, 2046 (1991).
- [3] M. Srednicki, *Phys. Rev. E* **50**, 888 (1994).
- [4] M. Srednicki, *J. Phys. A* **29**, L75 (1996).
- [5] M. Srednicki, *J. Phys. A* **32**, 1163 (1999).
- [6] M. Rigol, V. Dunjko, V. Yurovsky, and M. Olshanii, *Phys. Rev. Lett.* **98**, 050405 (2007).
- [7] A. Iucci and M. A. Cazalilla, *Phys. Rev. A* **80**, 063619 (2009).
- [8] P. Calabrese, F. H. L. Essler, and M. Fagotti, *J. Stat. Mech.* , P07016 (2012).
- [9] T. Barthel and U. Schollwöck, *Phys. Rev. Lett.* **100**, 100601 (2008).
- [10] M. Cramer, C. M. Dawson, J. Eisert, and T. J. Osborne, *Phys. Rev. Lett.* **100**, 030602 (2008).
- [11] M. Cramer and J. Eisert, *New J. Phys.* **12**, 055020 (2010).
- [12] D. Fioretto and G. Mussardo, *New J. Phys.* **12**, 055015 (2010).
- [13] P. Calabrese, F. H. L. Essler, and M. Fagotti, *Phys. Rev. Lett.* **106**, 227203 (2011).
- [14] P. Calabrese, F. H. L. Essler, and M. Fagotti, *J. Stat. Mech.* , P07022 (2012).
- [15] J.-S. Caux and R. M. Konik, *Phys. Rev. Lett.* **109**, 175301 (2012).
- [16] M. Collura, S. Sotiriadis, and P. Calabrese, *Phys. Rev. Lett.* **110**, 245301 (2013).
- [17] E. H. Lieb and D. W. Robinson, *Commun. Math. Phys.* **28**, 251 (1972).
- [18] R. Sims and B. Nachtergaele, *Lieb-Robinson bounds in quantum many-body physics*, edited by R. Sims and D. Ueltschi, Entropy and the Quantum, Vol. 529 (American Mathematical Society, 2010).
- [19] J. Jünemann, A. Cadarso, D. Perez-Garcia, A. Bermudez, and J. J. Garcia-Ripoll, *Phys. Rev. Lett.* **111**, 230404 (2013).
- [20] E. H. Lieb and A. Vershynina, arXiv:1306.0546v1 (2013).
- [21] M. Kliesch, C. Gogolin, and J. Eisert, *Lieb-Robinson bounds and the simulation of time evolution of local observables in lattice systems*, edited by L. D. Site and Bach, Many-Electron Approaches in Physics, Chemistry and Mathematics: A Multidisciplinary View (Springer, 2013).
- [22] D. Poulin, *Phys. Rev. Lett.* **104**, 190401 (2010).
- [23] S. Bravyi, M. B. Hastings, and F. Verstraete, *Phys. Rev. Lett.* **97**, 050401 (2006).
- [24] P. Calabrese and J. Cardy, *Phys. Rev. Lett.* **96**, 136801 (2006).
- [25] P. Calabrese and J. Cardy, *J. Stat. Mech.* , P04010 (2005).
- [26] P. Calabrese and J. Cardy, *J. Stat. Mech.: T* , P06008 (2007).
- [27] G. De Chiara, S. Montangero, P. Calabrese, and R. Fazio, *J. Stat. Mech.* , P03001 (2006).
- [28] A. Läuchli and C. Kollath, *J. Stat. Mech.* , P05018 (2008).
- [29] S. R. Manmana, S. Wessel, R. M. Noack, and A. Muramatsu, *Phys. Rev. B* **79**, 155104 (2009).
- [30] P. Hauke and L. Tagliacozzo, *Phys. Rev. Lett.* **111**, 207202 (2013).
- [31] J. Eisert, M. van den Worm, S. R. Manmana, and M. Kastner, *Phys. Rev. Lett.* **111**, 260401 (2013).
- [32] G. Carleo, F. Becca, L. Sanchez-Palencia, S. Sorella, and M. Fabrizio, *Phys. Rev. A* **89**, 031602 (2014).
- [33] M. Cheneau, P. Barmettler, D. Poletti, H. Endres, P. Schauß, T. Fukuhara, C. Gross, I. Bloch, C. Kollath, and S. Kuhr, *Nature* **481**, 484 (2012).
- [34] T. Langen, R. Geiger, M. Kuhnert, B. Rauer, and J. Schmiedmayer, *Nature Physics* **9**, 640 (2013).
- [35] P. Jurcevic, B. P. Lanyon, P. Hauke, C. Hempel, P. Zoller, R. Blatt, and C. F. Roos, arXiv:1401.5387 (2014).
- [36] P. Richerme, Z.-X. Gong, A. Lee, C. Senko, J. Smith, M. Moss-Feig, S. Michalakis, A. V. Gorshkov, and C. Monroe, arXiv:1401.5088 (2014).
- [37] C. Karrasch, J. E. Moore, and F. Heidrich-Meisner, *Phys. Rev. B* **89**, 075139 (2014).
- [38] S. R. White, *Phys. Rev. Lett.* **102**, 190601 (2009).
- [39] E. M. Stoudenmire and S. R. White, *New J. Phys.* **12**, 055026 (2010).
- [40] Note that the system is *not* connected to a heat bath during the time evolution and energy $\text{Tr}[H\rho(t)]$ is conserved.
- [41] P. Barmettler, D. Poletti, M. Cheneau, and C. Kollath, *Phys. Rev. A* **85**, 053625 (2012).
- [42] J.-S. Caux and F. H. L. Essler, *Phys. Rev. Lett.* **110**, 257203 (2013).
- [43] J. Mossel and J.-S. Caux, *J. Phys. A* **45**, 255001 (2012).
- [44] E. Demler and A. M. Tsvelik, *Phys. Rev. B* **86**, 115448 (2012).
- [45] M. P. Grabowski and P. Mathieu, *Ann. Phys.* **243**, 299 (1995).
- [46] T. Prosen and E. Ilievski, *Phys. Rev. Lett.* **111**, 057203 (2013).
- [47] B. Pozsgay, *J. Stat. Mech.* , P07003 (2013).
- [48] M. Fagotti and F. H. L. Essler, *J. Stat. Mech.* , P07012 (2013).
- [49] M. Fagotti, M. Collura, F. H. L. Essler, and P. Calabrese, *Phys. Rev. B* **89**, 125101 (2014).
- [50] B. Wouters, M. Brockmann, J. De Nardis, D. Fioretto, and J.-S. Caux, arXiv:1405.0172 (2014).
- [51] B. Pozsgay, M. Mestyán, M. A. Werner, M. Kormos, G. Zaránd, and G. Takás, arXiv:1405.2843 (2014).
- [52] B. Pozsgay, *J. Stat. Mech.* , P01011 (2011).
- [53] A. C. Cassidy, C. W. Clark, and M. Rigol, *Phys. Rev. Lett.* **106**, 140405 (2011).
- [54] M. Takahashi and M. Suzuki, *Prog. Theor. Phys.* **48**, 2187 (1972).
- [55] M. Fagotti and F. H. L. Essler, *Phys. Rev. B* **87**, 245107 (2013).
- [56] G. Vidal, *Phys. Rev. Lett.* **91**, 147902 (2003).
- [57] A. E. Feiguin and S. R. White, *Phys. Rev. B* **72**, 220401 (2005).
- [58] T. Barthel, U. Schollwöck, and S. R. White, *Phys. Rev. B* **79**, 245101 (2009).
- [59] C. Karrasch, J. H. Bardarson, and J. E. Moore, *Phys. Rev. Lett.* **108**, 227206 (2012).
- [60] T. Barthel, *New J. Phys.* **15**, 073010 (2013).
- [61] C. Karrasch, J. H. Bardarson, and J. E. Moore, *New J. Phys.* **15**, 083031 (2013).
- [62] M. Zwolak and G. Vidal, *Phys. Rev. Lett.* **93**, 207205 (2004).
- [63] F. Verstraete, J. J. Garcia-Ripoll, and J. I. Cirac, *Phys. Rev. Lett.* **93**, 207204 (2004).
- [64] T. Prosen and M. Žnidarič, *J. Stat. Mech.* , P07020 (2010).
- [65] R. J. Bursill, T. Xiang, and G. A. Gehring, *J. Phys.: Condens. Matter* **8**, L583 (1996).
- [66] X. Wang and T. Xiang, *Phys. Rev. B* **56**, 5061 (1997).
- [67] J. Sirker and A. Klümper, *Phys. Rev. B* **71**, 241101 (2005).

- [68] It is possible to evaluate observables that commute with the projection operator using the CPS rather than the METTS. The real time evolution, though, prohibits us from taking advantage of this improved measurement scheme.
- [69] D. Gobert, C. Kollath, U. Schollwöck, and G. Schütz, *Phys. Rev. E* **71**, 036102 (2005).
- [70] L. Bonnes and A. M. Läuchli, (in preparation) (2014).
- [71] M. Ganahl, E. Rabel, F. H. L. Essler, and H. G. Evertz, *Phys. Rev. Lett.* **108**, 077206 (2012).

Supplementary Material for “Light-cone” dynamics after quantum quenches in spin chains

Lars Bonnes,^{1,*} Fabian H. L. Essler,² and Andreas M. Läuchli¹

¹*Institute for Theoretical Physics, University of Innsbruck, A-6020 Innsbruck, Austria.*

²*The Rudolf Peierls Centre for Theoretical Physics, Oxford University, Oxford OX1 3NP, UK*

(Dated: August 29, 2014)

I. GENERALIZED THERMODYNAMIC BETHE ANSATZ

It is by now widely accepted, that at late time after the quench local properties of the spin-1/2 Heisenberg XXZ chain are described by a generalized Gibbs ensemble^{1,2}. The latter is constructed from the local integrals of motion $\{I_n\}$, where we take I_1 to be equal to the Hamiltonian. The set $\{I_n\}$ supposedly contains both the “ultra-local” integrals of motion obtained by taking logarithmic derivatives of the transfer matrix at the shift-point^{3,4}, and the “quasi-local” operators discovered recently⁵. The GGE density matrix is of the form

$$\rho_{\text{GGE}} = \frac{1}{Z_{\text{GGE}}} e^{-\sum_{n=1} \lambda_n I_n}, \quad (1)$$

where $Z_{\text{GGE}} = \text{Tr} e^{-\sum_{n=1} \lambda_n I_n}$ and the Lagrange multipliers λ_n are fixed by the requirements

$$i_n \equiv \lim_{L \rightarrow \infty} \frac{1}{L} \text{Tr}[\rho(t=0) I_n] = \lim_{L \rightarrow \infty} \frac{1}{L} \text{Tr}[\rho_{\text{GGE}} I_n]. \quad (2)$$

A practical way of constructing the GGE density matrix proceeds by first retaining a given number n_0 of the most local conservation laws, giving rise to a “truncated GGE”⁶ in the thermodynamic limit, and then increasing this number until the quantity of interest ceases to depend on n_0 . In the thermodynamic limit the density matrix ρ_{GGE} is dominated by a saddle point, characterized as a the minimum of the generalized thermodynamic potential

$$G = \sum_{n=1}^{\infty} \lambda_n H^{(n)} - S, \quad (3)$$

where S is the entropy. For integrable models this saddle point macro-state can be determined by a generalized thermodynamic Bethe Ansatz⁷. The necessary analysis is very similar to the one for the thermal case, which is discussed in detail in the monograph [8]. In the following we first summarize some results of the analysis for the thermal case, and then present the modifications necessary to describe the GGE.

A. Structure of eigenstates

In order to conform to the notations of Ref. [8] we consider the Hamiltonian in the form

$$H(J, \Delta) = -J \sum_{j=1}^L S_j^x S_{j+1}^x + S_j^y S_{j+1}^y + \Delta S_j^z S_{j+1}^z, \quad (4)$$

and parametrize the anisotropy as

$$\cos \gamma = -\Delta. \quad (5)$$

We note that $H(J, \Delta)$ and $H(-J, -\Delta)$ are unitarily equivalent. Eigenstates of (4) can be labelled by N complex spectral parameters x_j , where N is the number of down spins

$$|x_1, \dots, x_N\rangle. \quad (6)$$

Energy and momentum of these states are⁸

$$E = \sum_{j=1}^N J \frac{\sin^2 \gamma}{\cos \gamma - \cosh \gamma x_j} - \frac{N \Delta J}{4},$$

$$P = \sum_{j=1}^N i \ln \left[-\frac{\sinh \frac{\gamma}{2} (x_j + i)}{\sinh \frac{\gamma}{2} (x_j - i)} \right] \equiv \sum_{j=1}^N p^{(0)}(x_j). \quad (7)$$

Imposing periodic boundary conditions leads to the Bethe Ansatz equations

$$\left[\frac{\sinh \frac{\gamma}{2} (x_j + i)}{\sinh \frac{\gamma}{2} (x_j - i)} \right]^L = \prod_{l \neq j}^N \left[\frac{\sinh \frac{\gamma}{2} (x_j - x_l + 2i)}{\sinh \frac{\gamma}{2} (x_j - x_l - 2i)} \right],$$

$$j = 1, 2, \dots, N. \quad (8)$$

An important feature of integrable models like the Heisenberg XXZ chain is that excitations over the ground state are composed of different types of “elementary” excitations, corresponding to particular “string” patterns of rapidities in the complex plane, the precise structure of which depends on the anisotropy parameter Δ ⁸. In order to keep things simple, in the following we focus on particular values of Δ

$$\Delta_\ell = -\cos(\pi/\ell), \quad \ell = 1, 2, \dots \quad (9)$$

For these values there are ℓ types of excitations⁸

- positive parity 1-strings, corresponding to real roots x_j^1 of (8).

- negative parity 1-strings, corresponding to roots x_j^ℓ of (8) with imaginary part equal to ℓ .
- positive parity n -strings for $2 \leq n \leq \ell - 1$. These correspond to solutions of (8) such that

$$x_{\alpha,j}^n = x_\alpha^n + i(n+1-2j), \quad j = 1, \dots, n, \quad x_\alpha^n \in \mathbb{R}. \quad (10)$$

Substituting this “string hypothesis” back in the Bethe Ansatz equations (8) and taking the logarithm leads to a set of coupled equations for the string centres known as “discrete Takahashi equations” (DTE) for a solution with M_j strings of type j

$$L\theta_j(x_\alpha^j) - \sum_{k=1}^{\ell} \sum_{\beta=1}^{M_k} \Theta_{j,k}(x_\alpha^j - x_\beta^k) = 2\pi I_\alpha^j, \quad \alpha = 1, \dots, M_j, \quad j = 1, \dots, \ell. \quad (11)$$

Here I_α^j are integer or half-odd integer numbers,

$$\theta_j(x) = \begin{cases} 2 \arctan \left[\cot \left(\frac{\pi j}{2\ell} \right) \tanh \left(\frac{\pi x}{2\ell} \right) \right] & \text{if } j \neq \ell \\ -2 \arctan \left[\tan \left(\frac{\pi}{2\ell} \right) \tanh \left(\frac{\pi x}{2\ell} \right) \right] & \text{if } j = \ell. \end{cases}$$

$$\Theta_{j,k}(x) = \theta_{k-j}(x) + 2 \sum_{r=1}^{j-1} \theta_{k-j+2r}(x) + \theta_{k+j}(x), \quad \text{if } j \leq k < \ell, \quad (12)$$

and $\Theta_{j,k}(x) = \Theta_{k,j}(x)$, $\Theta_{j,\ell}(x) = -\Theta_{j,\ell-1}(x)$. Energy and momentum of solutions of the DTE are given by

$$E = -N \frac{J\Delta}{4} + \sum_{j=1}^{\ell} \sum_{\alpha=1}^{M_j} \epsilon_j^{(0)}(x_\alpha^j),$$

$$P = \sum_{j=1}^{\ell} \sum_{\alpha=1}^{M_j} \frac{2\pi I_\alpha^j}{L}, \quad (13)$$

where the bare energies are of the form

$$\epsilon_j^{(0)}(x) = -\frac{2\pi J \sin \gamma}{\gamma} a_j(x), \quad (14)$$

$$a_j(x) = \frac{1}{2\pi} \frac{\gamma \sin(\gamma q_j)}{\cosh(\gamma x) + \cos(\gamma q_j)}. \quad (15)$$

Here the parameters q_j are given by

$$q_j = \ell - j, \quad j \leq \ell - 1, \quad q_\ell = -1. \quad (16)$$

B. TBA equations for the XXZ chain at finite temperature

At temperature $T > 0$ the state of thermodynamic equilibrium is characterized by root densities $\rho_j^{p,h}$ describing the distributions of “particles” and “holes” of these different types of elementary excitations. The

densities are determined from the following systems of equations⁸

$$\frac{\epsilon_j(x)}{T} = \frac{\epsilon_j^{(0)}(x)}{T} + \sum_{k=1}^{\ell} \text{sgn}(q_k) T_{jk} * \ln \left[1 + e^{-\epsilon_k/T} \right] \Big|_x,$$

$$a_j(x) = \text{sgn}(q_j) [\rho_j^p(x) + \rho_j^h(x)] + \sum_k T_{jk} * \rho_k^p \Big|_x, \quad (17)$$

where the dressed energies $\epsilon_j(x)$ are defined as

$$\epsilon_j(x) = T \ln \left[\frac{\rho_j^h(x)}{\rho_j^p(x)} \right]. \quad (18)$$

The operation $*$ denotes convolution, e.g.

$$T_{jk} * \rho_k^p \Big|_x = \int_{-\infty}^{\infty} dy T_{jk}(x-y) \rho_k^p(y), \quad (19)$$

and the Fourier transforms of the integral kernels are given by ($T_{jk}(x) = T_{kj}(x)$)

$$\tilde{T}_{jk}(\omega) = \delta_{j,\ell-1} \delta_{k,\ell} - \delta_{j,k} + 2 \text{sgn}(q_j) \coth(\omega) \times \frac{\sinh((\ell - |q_j|)\omega) \sinh(q_k \omega)}{\sinh(\ell \omega)}, \quad j \leq k. \quad (20)$$

Given a solution of the TBA equations (17) we can for example calculate the free energy per site

$$f = -\frac{J\Delta}{4} - \sum_n \int dx a_n(x) \ln \left[1 + e^{-\epsilon_n(x)/T} \right] \text{sgn}(q_n). \quad (21)$$

C. Generalized Gibbs Ensembles

The analysis for the GGE closely parallels the thermal case. The Bethe Ansatz states are simultaneous eigenstates of the Hamiltonian and the higher conservation laws, and as a result we have ($m = 2, 3, \dots$)

$$I_m |x_1, \dots, x_N\rangle = \left[\sum_{j=1}^N \nu_m^{(0)}(x_j) \right] |x_1, \dots, x_N\rangle. \quad (22)$$

For the standard set of ultra-local conservation laws we have¹⁰

$$\nu_m^{(0)}(x) = J \left(\frac{\sin \gamma}{\gamma} \frac{\partial}{\partial x} \right)^{m-1} \frac{\sin^2 \gamma}{\cos \gamma - \cosh \gamma x}. \quad (23)$$

Minimizing the generalized Gibbs free energy⁷ of the truncated GGE⁶

$$G_{n_0} = \sum_{n=1}^{n_0} \lambda_n H^{(n)} - S, \quad (24)$$

where S is the entropy, leads to the generalized TBA equations

$$\begin{aligned} \epsilon_j(x) &= \epsilon_j^{(0)}(x) + \sum_{k=1}^{\ell} \text{sgn}(q_k) T_{jk} * \ln [1 + e^{-\epsilon_k}] \Big|_x, \\ a_j(x) &= \text{sgn}(q_j) [\rho_j^p(x) + \rho_j^h(x)] + \sum_{k=1}^{\ell} T_{jk} * \rho_k^p \Big|_x, \end{aligned} \quad (25)$$

where now

$$\begin{aligned} \epsilon_j^{(0)}(x) &= \sum_{n=1}^{n_0} \lambda_n \nu_{n,j}^{(0)}(x), \\ \nu_{n,j}^{(0)}(x) &= \left(\frac{\sin \gamma}{\gamma} \frac{\partial}{\partial x} \right)^{n-1} \epsilon_j^{(0)}(x), \end{aligned} \quad (26)$$

and the relation to particle and hole densities is

$$\frac{\rho_j^h(x)}{\rho_j^p(x)} = e^{\epsilon_j(x)}. \quad (27)$$

The generalized TBA equations (25) have a form that is similar to the finite temperature ones (17). However, the ‘‘driving terms’’ $\epsilon_j^{(0)}(\lambda)$ are different in the two cases, and this leads to significant differences in the solutions $\epsilon_j(x)$ in the two cases.

Eqns (25) characterize the saddle point state of the density matrix (1). In order to obtain the correct representative state for our given initial conditions, we have to fix the Lagrange multipliers λ_j such that the constraints (2) are fulfilled. Given a set of distribution functions for particles, the expectation values of the conservation laws can be calculated

$$i_m = \lim_{L \rightarrow \infty} \frac{\langle I_m \rangle}{L} = \sum_{j=1}^{\ell} \int dx \nu_{m,j}^{(0)}(x) \rho_j^p(x). \quad (28)$$

In practice we characterize the initial density matrix by computing $\{i_m\}$ numerically, and we are therefore restricted to retaining only very few (one or two) higher conservation laws. Given the expectation values $\{i_m\}$ we then solve the generalized TBA equations (25) under the constraints

$$i_m - \sum_{j=1}^{\ell} \int dx \nu_{m,j}^{(0)}(x) \rho_j^p(x) = 0, \quad (29)$$

self-consistently by iteration.

D. ‘‘Excitations’’ over the GGE equilibrium state

Once we have obtained a solution $\{\rho_j^{p,h}(x)\}$, we may construct a particular eigenstate (‘‘representative state’’⁹) of the Hamiltonian that gives rise to these densities in the thermodynamic limit, i.e. go to an appropriate

microcanonical ensemble. This eigenstate is characterized by a solution of the DTE (11) for a particular set of (half-odd) integer numbers I_{α}^j

$$L\theta_j(x_{\alpha}^j) - \sum_{k=1}^{\ell} \sum_{\beta=1}^{M_k} \Theta_{j,k}(x_{\alpha}^j - x_{\beta}^k) = 2\pi I_{\alpha}^j. \quad (30)$$

Energy and momentum of this state are given by (13)

$$E_0 = \sum_{j=1}^{\ell} \sum_{\alpha=1}^{M_j} \epsilon_j^{(0)}(x_{\alpha}^j), \quad P_0 = \sum_{j=1}^{\ell} \sum_{\alpha=1}^{M_j} \frac{2\pi I_{\alpha}^j}{L}. \quad (31)$$

We may now construct ‘‘excitations’’ over this eigenstate by standard techniques. Small changes in the I_{α}^j give rise to solutions $\{\tilde{x}_{\alpha}^j\}$ of the DTE, which are very similar to the solution $\{x_{\alpha}^j\}$ for the representative state. For our purposes it is sufficient to consider a single particle-hole excitation for m -strings, because energies and momenta are additive. This corresponds to a solution where all (half-odd) integers are the same as for the representative state, except for m -strings, where one of the (half-odd) integers, denoted by I_h^m , is replaced by I_p^m . The corresponding DTE read

$$\begin{aligned} L\theta_j(\tilde{x}_{\alpha}^j) - \sum_{k=1}^{\ell} \sum_{\beta=1}^{M_k} \Theta_{j,k}(\tilde{x}_{\alpha}^j - \tilde{x}_{\beta}^k) \\ = \Theta_{j,m}(\tilde{x}_{\alpha}^j - x_p^m) - \Theta_{j,m}(\tilde{x}_{\alpha}^j - x_h^m) + 2\pi I_{\alpha}^j. \end{aligned} \quad (32)$$

In addition there are the equations determining the precise positions $x_{p,h}^m$ of the particle and the hole, but we do not need them here. Energy and momentum of this state are given by (13)

$$E = \sum_{j=1}^{\ell} \sum_{\alpha=1}^{M_j} \epsilon_j^{(0)}(\tilde{x}_{\alpha}^j), \quad P = P_0 + I_p^m - I_h^m. \quad (33)$$

In order to work out the differences $\Delta E(x_p^m, x_h^m) = E - E_0$ and $\Delta P(x_p^m, x_h^m) = P - P_0$ it is useful to introduce shift-functions³

$$F_j(x_{\alpha}^j) \equiv \frac{x_{\alpha}^j - \tilde{x}_{\alpha}^j}{x_{\alpha+1}^j - \tilde{x}_{\alpha}^j}. \quad (34)$$

Taking the difference between (30) and (32) and then going over to the thermodynamic limit we obtain a set of *linear* integral equations for the shift functions

$$\begin{aligned} F_j(x) \text{sgn}(q_j) \left[1 + e^{\epsilon_j(x)} \right] + \sum_k T_{jk} * F_k \Big|_x \\ = \frac{1}{2\pi} [\Theta_{j,m}(x - x_p^m) - \Theta_{j,m}(x - x_h^m)]. \end{aligned} \quad (35)$$

A useful short-hand notation for this system of equations is

$$F_j(x) - \sum_k K_{jk} * F_k \Big|_{x_j} = f_j^{(0)}(x), \quad (36)$$

where we have defined

$$f_j^{(0)}(x) = \frac{\text{sgn}(q_j)}{2\pi} \frac{\Theta_{j,m}(x-x_p^m) - \Theta_{j,m}(x-x_h^m)}{1 + e^{\epsilon_j(x)}},$$

$$K_{jk}(x,y) = -\text{sgn}(q_j) \frac{T_{jk}(x-y)}{1 + e^{\epsilon_j(x)}}. \quad (37)$$

We may write down a formal solution of the set of integral equations by inverting (36)

$$F_j(x) = (I - K)_{jk}^{-1} * f_k^{(0)} \Big|_x. \quad (38)$$

The ‘‘excitation energy’’ is then

$$\Delta E(x_p^m, x_h^m) = \epsilon_m^{(0)}(x_p^m) - \epsilon_m^{(0)}(x_h^m) + \sum_k \int dx_k (\epsilon_k^{(0)}(x_k))' F_k(x_k). \quad (39)$$

The second line is rewritten as

$$\sum_k \int dx_k (\epsilon_k^{(0)}(x_k))' (I - K)_{kj}^{-1} * f_j^{(0)} \Big|_{x_k}. \quad (40)$$

We now define functions $e'_j(x)$ by

$$e'_j * (I - K)_{jk} \Big|_{x_k} = (\epsilon_k^{(0)}(x_k))'. \quad (41)$$

Inverting the integral operator gives

$$e'_j(x_j) = (\epsilon_m^{(0)})' * (I - K)_{mj} \Big|_{x_j}, \quad (42)$$

which in turn allows us to recast expression (39) for the energy difference in the form

$$\Delta E(x_p^m, x_h^m) = \epsilon_m^{(0)}(x_p^m) - \epsilon_m^{(0)}(x_h^m) + \int dx_j e'_j(x_j) f_j^{(0)}(x_j). \quad (43)$$

Finally, using that

$$\frac{\partial f_j^{(0)}(x_j)}{\partial x_p^m} = K_{jm}(x_j, x_p^m), \quad (44)$$

we obtain

$$\frac{\partial \Delta E(x_p^m, x_h^m)}{\partial x_p^m} = e'_m(x_p^m). \quad (45)$$

This allows us to express the energy in the form

$$\Delta E(x_p^m, x_h^m) = e_m(x_p^m) - e_m(x_h^m). \quad (46)$$

The momentum of the excitation is simply

$$\Delta P(x_p^m, x_h^m) = \frac{2\pi}{L} (I_p^m - I_h^m) = z_m(x_p^m) - z_m(x_h^m), \quad (47)$$

where $z_m(x)$ is the counting function for m -strings. The counting functions can be obtained from a set of coupled, nonlinear integral equations, but for our purposes it suffices that

$$\frac{dz_j(x)}{dx} = 2\pi [\rho^p(x) + \rho^h(x)]. \quad (48)$$

The conclusion of these considerations is that the particle contributes $e_m(x_p^m)$ to the energy and $z_m(x_p^m)$ to the momentum. Furthermore, contributions from particles and holes are additive. The group velocity of the particle is then given by

$$v_m(x) = \frac{\partial e_m(x)}{\partial z_m(x)} = \frac{\frac{\partial e_m(x)}{\partial x}}{\frac{\partial z_m(x)}{\partial x}} = \frac{e'_m(x)}{2\pi \rho_m^p(x) (1 + e^{\epsilon_m(x)})}. \quad (49)$$

In order to determine the velocities of the various elementary excitations, we first solve the gTBA equations as described above, substitute the solution for the dressed energies into the integral equations (41) for the functions $e'_j(x)$, and finally solve the latter numerically by iteration.

II. FINITE-TEMPERATURE TIME EVALUATING USING METTS

The idea of minimally entangled typical thermal states, put forward by White¹¹, is to devise a Markov process to importance sample wave functions such that *i*) the ensemble average of the expectation values of some operator equals the expectation value with respect to a thermal (Gibbs) ensemble and *ii*) the entanglement entropy of the sampled wave functions is small such that they can be represented efficiently via matrix product states. We will briefly review the algorithm which is detailed in Refs. 11,12 and comment on the implementation of the time evolution.

To be specific, consider the expectation value of some operator with respect to the thermal density matrix $\rho_\beta = 1/Z \exp(-\beta H)$, where $Z = \text{tr}[\exp(-\beta H)]$ is the partition function and $\beta = 1/(k_B T)$ is the inverse temperature. It reads

$$\langle \hat{O} \rangle_\beta = \text{tr}[\hat{O} \rho_\beta] = \frac{1}{Z} \sum_{\vec{i}} \langle \vec{i} | e^{-\beta H/2} \hat{O} e^{-\beta H/2} | \vec{i} \rangle \quad (50)$$

and can be expanded in an orthonormal basis $\{|\vec{i}\rangle\}$. One then defines a set of properly normalized states via the mapping

$$|\Psi_{\vec{i}}\rangle = \frac{e^{-\beta H/2} |\vec{i}\rangle}{\sqrt{\langle \vec{i} | e^{-\beta H} | \vec{i} \rangle}} \quad (51)$$

such that equation (50) is cast into the form

$$\langle \hat{O} \rangle_\beta = \sum_{\vec{i}} P(\vec{i}) \langle \Psi_{\vec{i}} | \hat{O} | \Psi_{\vec{i}} \rangle \quad (52)$$

where $P(\vec{i}) = \langle \vec{i} | e^{-\beta H} | \vec{i} \rangle$ can be considered as the ‘‘Boltzmann weight’’ of state $|\vec{i}\rangle$.

The idea of importance sampling is to generate states $|\Psi_{\vec{i}}\rangle$ with probability $P(\vec{i})$ such that the weighted sum in equation (52) can be approximated by an ensemble average over states

$$\langle \hat{O} \rangle_\beta \approx \overline{\langle \Psi_{\vec{i}} | \hat{O} | \Psi_{\vec{i}} \rangle}. \quad (53)$$

The METTS algorithm is then a Markov chain whose stationary distribution samples the states $|\Psi_{\vec{i}}\rangle$ with the correct distribution and the procedure works as follows^{11,12}:

1. Start from a random classical product state (CPS) $|\vec{i}\rangle$.
2. Evolve the CPS in imaginary time, $|\psi_{\vec{i}}\rangle = e^{-\beta H/2} |\vec{i}\rangle$.
3. Project back into a CPS basis with probability $p(i \rightarrow j) = \langle \psi_{\vec{i}} | \vec{j} \rangle$.
4. Continue with 2.

Eventually, the states $|\psi_{\vec{i}}\rangle$ will thermalize towards the correct METTS ensemble $|\Psi_{\vec{i}}\rangle$.

A couple of remarks are in order. First, the autocorrelation time of the Markov chain strongly depends on the CPS basis. In particular, the naive approach only projecting into the S_z basis (which would allow the efficient use of magnetization as a conserved quantity) is found to converge only extremely slowly. Projection into different bases such as alternating between the S_z and S_x basis restores ergodicity and helps the algorithm to properly explore the full phase space which results in a very fast thermalization¹¹. Second, the projection in step 3. can be done without calculating all overlaps (which would take exponentially long) but can be implemented using a successive projection using matrix product operators as detailed in Ref. 12.

To implement the quench we first generate the ensemble of METTS by starting from random CPS and applying the previously outlined projection procedure. For each state, we use a statistically independent random CPS initial state to avoid autocorrelation effects. The expectation values of the operators after the quench are then evaluated via the operator $\hat{O}(t)$ evolved in time with respect to the final Hamiltonian $H(\Delta_f)$. Inserting this into equation (53) yields

$$\langle \hat{O}(t) \rangle_\beta \approx \overline{\langle \Psi_{\vec{i}} | e^{iH(\Delta_f)t} \hat{O} e^{-iH(\Delta_f)t} | \Psi_{\vec{i}} \rangle}. \quad (54)$$

This means that we have evolve each state of our METTS ensemble in time (we do so by using the standard TEBD¹³ algorithm) and are then able to calculate ensemble averages over the evolved ensemble at each time step.

* Electronic address: lars.bonnes@uibk.ac.at

¹ M. Fagotti and F.H.L. Essler, J. Stat. Mech. P07012 (2013); M. Fagotti, M. Collura, F.H.L. Essler and P. Calabrese, Phys. Rev. B **89**, 125101 (2014).

² M. Rigol, V. Dunjko, V. Yurovsky, and M. Olshanii, Phys. Rev. Lett. **98**, 50405 (2007).

³ V.E. Korepin, A.G. Izergin, and N.M. Bogoliubov, *Quantum Inverse Scattering Method, Correlation Functions and Algebraic Bethe Ansatz* Cambridge University Press, 1993;

⁴ M. P. Grabowski and P. Mathieu, Annals Phys. **243**, 299 (1995).

⁵ T. Prosen and E. Ilievski, Phys. Rev. Lett. **111**, 057203 (2013).

⁶ M. Fagotti and F.H.L. Essler, Phys. Rev. B **87**, 245107

(2013).

⁷ J.-S. Caux and J. Mossel, J. Phys. A: Math. Theor. **45**, 255001 (2012).

⁸ M. Takahashi, *Thermodynamics of One-Dimensional Solvable Models*, Cambridge University Press, Cambridge 1999.

⁹ J.-S. Caux and F.H.L. Essler, Phys. Rev. Lett. **110**, 257203 (2013).

¹⁰ N. Muramoto and M. Takahashi, J. Phys. Soc. Jpn **68**, 2098 (1999).

¹¹ S. R. White, Phys. Rev. Lett. **102**, 190601 (2009)

¹² E. M. Stoudenmire and S. R. White, New. J. Phys. **12**, 055026 (2010).

¹³ G. Vidal, Phys. Rev. Lett. **91**, 147902 (2003)

